Impact of sub-grid scale models on resolving mixing and thermal shear layers in Large Eddy Simulation of JHC flames

Javad Aminian[a,*], Chiara Galletti[b], Leonardo Tognotti[b]

[a] *Optimization of Energy Systems Lab., Faculty of Mechanical and Energy Engineering, Shahid Beheshti University, A.C., Tehran, Iran*

[b] *Department of Civil and Industrial Engineering, University of Pisa, Pisa, Italy*

Abstract

Predictive performance of sub-grid scale (SGS) models is investigated in Large Eddy Simulation (LES) of a methane/hydrogen jet-in-hot coflow (JHC) flame using a conceptual analysis proposed for the mean values of major combustion products. It is shown that mean values of major combustion products consist of valuable information on several characteristics of JHC flames such as flame thickness, flame volume and reaction intensity. In particular, sudden change of CO_2 and H_2O mass fractions from coflow contents to higher values, predicted by static SGS models, demonstrated a thin flame constricted around the center line. However, uniform ascending manner of CO_2 and H_2O contents in the coflow region predicted by dynamic SGS models revealed their ability on capturing characteristics of a distributed volumetric flame. For the temperature fluctuations in shear layers, the dynamic Smagorinsky model is also shown to provide better predictions than the constant-coefficient Smagorinsky model, the latter exhibiting significant over-predictions. It is also observed that the dynamic kinetic energy SGS model with its unique assumption of non-equilibrium turbulence is the best fitted SGS model for the JHC

[*]Corresponding Author: j_aminian@sbu.ac.ir (J. Aminian)

Phone: +98 (021) 7393 2693, Fax: +98 (021) 7731 1446,

flames as it provides improved accuracy on developing mixing and thermal shear layers by solving an extra transport equation for turbulent kinetic energy.

Keywords: Conceptual analysis; mean values of major combustion products; sub-grid scale models; methane/hydrogen JHC flame; shear layers

NOMENCLATURES

C_s, C_k, C_ε	Empirical model constants	z	Axial coordinate
k	Kinetic energy	Z	Mixture fraction
p	Pressure		
r	Reaction rate	**Greek letters**	
rms	Fluctuating property	ϑ	Kinematic viscosity
S_{ij}	Strain tensor	τ_{ij}	Sub-grid scale stress tensor
t	Time	Δ	Grid filter length
T	Temperature	δ_{ij}	Kronecker delta
T_{ij}	Test filter stress tensor	Δt	Time spane
u	Velocity component	Δx	Step size
u'	Fluctuating velocity component	μ_{eff}	Effective dynamic viscosity
V	Volume of the computational cell	**Subscript**	
x_j	Space coordinates	t	Turbulent
Y	Species mass fraction	sgs	Sub-grid scale

1. Introduction

Developing new combustion technologies requires better understanding of turbulence-chemistry interaction, scalar mixing, vortex dynamics, combustion instability, local extinction and re-ignition. Analysis of these phenomena is practically important in the design of reduced emission technologies like the Moderate or Intense Low Oxygen Dilution (MILD) combustion in which enhanced recirculation of combustion products extends turbulent mixing of reactants

throughout the furnace [1]. Nowadays, the impact of large scale eddies in turbulent mixing and combustion is well accepted. On one hand, turbulent large structures can wrinkle the flame and even quench it and, on the other hand, they can improve heat transfer and mixing, thus increasing the efficiency of combustion devices. Large Eddy Simulation (LES) is properly suited for the prediction of these phenomena as it is based on a direct resolution of the large scales of turbulence, whereas it models the effect of smallest scales (known as sub-filter or sub-grid scales) which tend to be more universal and hence easier to model [2]. Direct resolving of large eddies forces one to use much finer mesh and smaller time step in LES than those commonly employed in classical Reynolds-Averaged Navier Stokes (RANS) techniques. The main advantage of LES over computationally cheaper RANS approaches is the increased level of details it can provide. While RANS approaches provide "averaged" results, LES is able to predict instantaneous flow characteristics. This is particularly important for mixing simulations in non-premixed combustion. It is worth noting that chemical reactions, in all diffusion and premixed flames, occur only when molecular mixing of fuel and oxidizer takes place in the smallest dissipative scales. Thus, the combustion phenomenon occurs essentially at the smallest sub-grid scales, which has to be modeled in LES. Therefore, accurate treatment of sub-grid scales has a substantial impact on combustion modeling [3].

The newly developed MILD combustion technology, that is also referred to as flameless oxidation (FLOX) [4], or high temperature air combustion (HiTAC) [5] is achieved by diluting and preheating the fuel and oxidizer streams to weaken the reaction zone while sustaining in a distributed zone with temperature above the mixture auto-ignition point. Because of the numerous attractive potentials of MILD combustion, *e.g.* reduced pollutant emission, enhanced thermal efficiency, silent operation and uniform temperature distribution, this technology suits

for multiple applications, such as thermal treatment processes, combustion of low calorific value fuels, hydrogen enriched fuels, biogases and industrial wastes, as well as gas turbines [6]. For that reason MILD combustion has been largely studied experimentally and numerically over the past decade [1, 3-9]. Among all, the experimental study of Dally and coworkers on MILD combustion of Jet-in-Hot-Coflow (JHC) flames [7] has received many attentions by modeling experts [9-13], mainly because of the high fidelity and accuracy of experimental data, consisting of in-flame measurements of temperature and species concentration.

Fig. 1 illustrates a schematic configuration of JHC flames. Dally *et al.* [7] were the first to study JHC flames with the objective of emulating MILD combustion conditions. These unconfined flames are complicated because of simultaneous occurrence of laminar and turbulent regions superimposed in hot and cold flow streams with scalar fluctuations in the mixing and thermal shear layers. As can be observed in Fig. 1, first part of the flame mimics vitiated MILD conditions as it receives deficient levels of oxygen from hot and diluted coflow stream. However, penetrating higher amounts of oxygen from atmospheric tunnel air into the reaction zone at downstream alters the MILD conditions to intense diffusion flame. Therefore, better fundamental understanding of MILD combustion in the configuration of JHC flames demands accurate resolving of mixing and thermal shear layers as a prerequisite to reasonably predict temperature and species fields in subsequent steps.

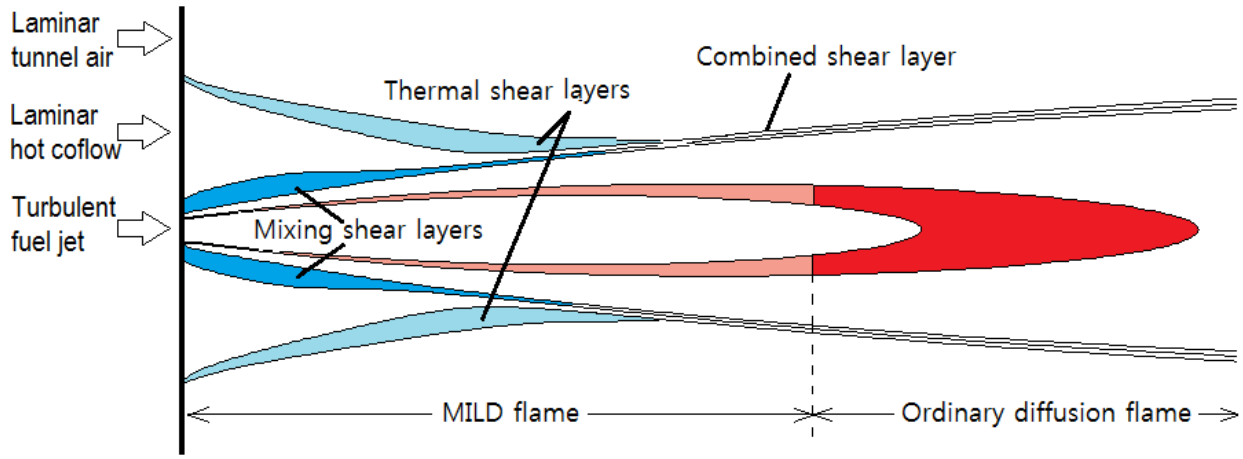

Fig. 1. Schematic configuration of JHC flames

Most of the numerical investigations employed the classical RANS turbulent closures to simulate JHC flames [11-13]. Aminian *et al.* [12] provided a critical description of the importance of well treating shear layers in JHC configurations; they demonstrated that improved prediction of minor species in JHC flames can be obtained only via direct resolving of temperature fluctuations in thermal and mixing shear layers.

Ihme and See [14] developed a three-stream flamelet/progress variable (FPV) model and employed it in LES to model characteristics of the HM3 flame of Dally's experiments. They argued that the inhomogeneous mixture composition of the coflow inlet is mainly responsible for difficulties in capturing flame characteristics of this burner. They obtained some success in predicting the overall trend of mean temperature, CO_2 and CO mass fractions as well as the temperature fluctuations in the fuel jet-coflow shear layer by introducing non-homogeneous scalar compositions at the coflow inlet using digital filter method proposed by Klein *et al.* [15]. However, peak flame temperature at distance of 30 and 60 mm from the burner and temperature fluctuation in the coflow-tunnel air shear layer showed some discrepancies with the experimental data. In another study, Ihme *et al.* [16] employed the previously developed three stream FPV

model with LES approach for prediction of HM3, HM2 and HM1 flames (9%, 6% and 3% O_2 mass fraction in the hot coflow). LES results and experiments were in good agreement for all three flame-configurations. Discrepancies for the carbon-containing species on the fuel-rich-side was however observed and concluded that further improvements can be obtained if time-dependent description of the inflow conditions is applied in boundaries. The influence of hydrogen addition to the Adelaide JHC flame was studied by Afarin and Tabejamaat [17] using a static SGS model based on the Yoshizawa formula. Using the mean profiles of temperature, formaldehyde and hydroxyl radicals they showed that increasing hydrogen content in fuel stream decreases the presence of premixed zones and damps OH oscillations. Zhang *et al.* performed LES modeling to investigate stabilization mechanism and combustion regime of the Cabra diffusion flame via a tabulated detailed chemistry combined with a PDF model. They showed that their proposed SGS model is able to accurately predict lift-off height in hot vitiated coflow flame. No particular discussion has been presented, however, for reasonable treating of mixing or thermal shear layers which is common in JHC flames [18]. Abtahizadeh *et al.* investigated effects of preferential diffusion in Large Eddy Simulation of turbulent lifted CH4/H2 flames. They demonstrated that preferential diffusion has a significant influence on the lift-off height and stabilization mechanism of the lifted H2-enriched turbulent flames. They also observed some discrepancies of velocity fluctuations in the transition region of the fuel jet stream and referred them to the inaccurate Smagorinsky SGS model [19]. Impact of SGS models on resolving characteristics of swirling diffusion flames was studied later by the Hu *et al.* [20]. They compared results of SL and Dynamic Kinetic Energy (DKE) SGS models and concluded that the DKE predictions on the flame shape and length is better than those obtained with the SL SGS model. Unlike the swirling diffusion flames which receive many attentions on LES modeling, no

attempt has yet been performed to investigate effects of SGS models on capturing the complex behavior of mixing and thermal shear layers in JHC flames.

Present study attempts to provide guidance for SGS modeling in the Large Eddy Simulation of JHC flames in which role of interconnecting mixing and thermal shear layers is significant. In particular, LES of the HM3 flame from the Adelaide JHC burner is performed aiming at investigating the effect of four static and dynamic SGS models on the prediction of fluctuating scalars in shear layers. In this regard, a conceptual analysis of the mean values of major combustion products is conducted in five steps to distinguish effect of SGS models in prediction of JHC flames characteristics. The main goal is to elucidate the impact of SGS models on the prediction of unsteady nature of scalar fluctuations in mixing and thermal shear layers.

2. LES modeling

Governing equations in LES are obtained by spatial filtering of the Navier-Stokes equation in order to separate the large scale structures (resolved scales) from the small or sub-grid scale eddies. In a finite volume discretization employed here, a filtered variable (denoted by an over-bar) based on a top-hat filter function is defined as:

$$\overline{\emptyset} = \frac{1}{V}\int_V \emptyset(y)dy \quad ; \quad y \in V \tag{1}$$

where, V is the volume of the computational cell which determines size of the resolved scales. The filtered Navier-Stokes equations for incompressible flows can then be written as:

$$\frac{\partial \overline{u}_i}{\partial t} + \frac{\partial \overline{u}_i \overline{u}_j}{\partial x_j} = -\frac{1}{\rho}\frac{\partial \overline{p}}{\partial x_j} - \frac{\partial \tau_{ij}}{\partial x_j} + \frac{\partial}{\partial x_j}\left(\vartheta \frac{\partial \overline{u}_i}{\partial x_j}\right) \tag{2}$$

The above filtering operation introduces the unknown τ_{ij} called sub-grid scale (SGS) stress tensor and leaves Eq. (2) unclosed. The SGS stresses are defined as:

$$\tau_{ij} \equiv \overline{u_i u_j} - \overline{u}_i \overline{u}_j \tag{3}$$

Models based on isotropic eddy-viscosity compute the SGS stresses through the Boussinesq hypothesis as:

$$\tau_{ij} - \frac{1}{3}\tau_{kk}\delta_{ij} = -2\vartheta_t \overline{S}_{ij} \quad (4)$$

where, τ_{kk} is the isotropic part of SGS stresses which is added to the filtered static pressure term and $\overline{S}_{ij}$ is the resolved rate of strain tensor defined as $\overline{S}_{ij} = 1/2\left(\partial\overline{u}_i/\partial x_j + \partial\overline{u}_j/\partial x_i\right)$. ϑ_t is the SGS eddy-viscosity and has to be determined to close Eq. (2). In this paper, the static Smagorinsky model with different constant values and two dynamic SGS models namely the dynamic Smagorinsky and dynamic kinetic energy models have been investigated starting with a brief description on their formulations and inherent assumptions.

2.1. Smagorinsky model

In the simple model proposed by Smagorinsky [21] it is assumed that the production and dissipation rates of turbulent energy are in equilibrium. This yields to an expression for eddy-viscosity based on Eq. (5).

$$\vartheta_t = C_s\overline{\Delta^2}\left|\overline{S}\right| \quad (5)$$

where, C_s is the model constant, $\overline{\Delta}$ is the grid filter length computed as $\overline{\Delta} = V^{1/3}$ and $\left|\overline{S}\right| = \left(2\overline{S}_{ij}\overline{S}_{ij}\right)^{1/2}$ is strain rate for the resolved scales. The Smagorinsky model is simple, economic and robust. Notwithstanding these merits, it has the well-known short coming that no single value of the model constant (C_s) is universally applicable to a wide range of flows. Several values have been proposed for the Smagorinsky constant. McMillan and Ferziger [22] stated that the correlation between turbulent stresses obtained from Smagorinsky model and DNS data is greatest when (C_s) is taken 0.17 recalling that for inertial sub-range a value of 0.17 should be considered for the Smagorinsky constant which is in agreement with Lilly [23] and Schumann

[24]. Higher values of C_s have been also proposed for isotropic turbulent flows [25]. In channel-flow calculations, however, a conservative value of 0.10 [26] or 0.065 [27] is proposed for the Smagorinsky constant. The Smagorinsky model is often too dissipative in nearly laminar regimes meaning that it yields a spurious low correlation (about 0.3) with the actual turbulent stress tensor in several flows [28, 29]. For the specific case of JHC configuration the fully turbulent flow switches to the transient and subsequently laminar flow as moving far from the axis. Hence, a specific choice of Smagorinsky constant may be appropriate for part of the flow while may bring erroneous predictions of turbulent stresses in other regions. This issue will be investigated in the present study by applying the standard (0.17) and conservative (0.10) values of the Smagorinsky constant.

2.2. Dynamic Smagorinsky model

Germano *et al.* [28] and Lilly [30] developed a procedure in which the Smagorinsky model constant is dynamically computed based on the information provided by the large eddies. The basic idea in dynamic Smagorinsky model is to consider the same Smagorinsky model at two different scales, and thus to adjust the constant accordingly. The dynamic procedure requires a "test" filter $\left(\tilde{\Delta}\right)$ to obtain small scales of the resolved field in advance. The test filter stress $\left(T_{ij}\right)$ associating with larger eddies is yet similar to the SGS stress $\left(\tau_{ij}\right)$ and therefore can be modeled according to the Boussinesq hypothesis:

$$T_{ij} - \frac{1}{3}T_{kk}\delta_{ij} = -2C_s\widetilde{\Delta^2}\left|\tilde{\bar{S}}\right|\tilde{\bar{S}}_{ij} \qquad (6)$$

In this model C_s varies in time and space and clipped between 0 (laminar flow) and 0.23 to avoid numerical instabilities. The dynamic Smagorinsky model can handle transitional flows and account for damping effects near wall boundaries.

2.3. Dynamic kinetic energy model

The underlying assumption of all models discussed previously is the local equilibrium between transferred and dissipated kinetic energy through the sub-grid scales. The sub-grid scale turbulence can be represented more faithfully by accounting for the transport of the SGS turbulent kinetic energy. Kim and Menon [31] proposed a transport model for the SGS turbulent kinetic energy which accounts for the history and non-local effects applicable to the complex flows with non-equilibrium turbulence. By contracting the sub-grid scale stress in Eq. (3) the SGS kinetic energy is defined as:

$$k_{sgs} = \frac{1}{2}\left(\overline{u_k^2} - \overline{u}_k^2\right) \tag{7}$$

The sub-grid scale eddy viscosity ϑ_t is then computed using k_{sgs} as follows:

$$\vartheta_t = C_k k_{sgs}^{1/2} \overline{\Delta} \tag{8}$$

where, k_{sgs} is obtained by solving its transport equation:

$$\frac{\partial k_{sgs}}{\partial t} + \frac{\partial \overline{u}_j k_{sgs}}{\partial x_j} = -\tau_{ij}\frac{\partial \overline{u}_i}{\partial x_j} - C_\varepsilon \frac{k_{sgs}^{3/2}}{\overline{\Delta}} + \frac{\partial}{\partial x_j}\left(\frac{\vartheta_t}{\sigma_k}\frac{\partial k_{sgs}}{\partial x_j}\right) \tag{9}$$

The first and second terms on the right hand of Eq. (9) stand for the SGS kinetic energy production and dissipation, respectively. Model constants appearing in Eqs. (8) and (9), namely C_k and C_ε, are determined dynamically [32] with turbulent Prandtl number σ_k set to 1. Non-local equilibrium assumption is the main superiority of the DKE model over the dynamic Smagorinsky model which allows transportation of turbulent kinetic energy through the flow (via Eq. (9)) and dissipation in another location. In the dynamic procedure towards determining C_k, both negative and positive values may be substituted in Eq. (8). A negative C_k and consequently negative eddy-viscosity is often interpreted as the flow of energy from the sub-grid scale eddies to the resolved eddies, referred to as "back-scattering", which is a desirable characteristic of the

dynamic models. This is another superiority of the dynamic kinetic energy model over the dynamic Smagorinsky model as negative eddy-viscosities in the dynamic Smagorinsky model are avoided due to numerical instabilities.

2.4. Summarizing SGS models characteristics

Overall comparison of the above reviewed SGS models is summarized in Table 1 based on three model characteristics. Model superiorities are highlighted compared to their weak points which left clear. In the upcoming sections we will examine these intrinsic model characteristics on predicting the MILD portion of Jet-in-Hot Coflow structures.

Table 1. Characteristics of static/dynamic sub-grid scale models

	Too dissipative	Dynamic assignment of model constant(s)	Non-local equilibrium
Smagorinsky ($C_s = 0.10$)	Yes/No	No	No
Smagorinsky ($C_s = 0.17$)	Yes/No	No	No
Dynamic Smagorinsky	No	Yes	No
Dynamic Kinetic Energy	No	Yes	Yes

3. Test case

The methane/hydrogen JHC flame referred to HM3 flame in the experimental study of Dally *et al.* [7] has been considered in the present study. This flame consists of CH_4/H_2 mixture (50-50 by vol.%) injected from a central nozzle (inner diameter ID = 4.25 mm), and surrounded by a vitiated and preheated coflow oxidizer (oxygen mass fraction $Y_{O_2} = 9\%$ and temperature $T = 1300$ K) introduced from a coaxial annulus (ID = 82 mm). The whole burner was placed in a wind tunnel which provided atmospheric air $\left(Y_{O_2} = 23\%\right)$ at ambient temperature ($T = 295$ K) to the flame zone with the same velocity of the coflow oxidizer ($u = 3.2\ m/s$). The fuel-jet was injected from the central feeding pipe at a Reynolds number of 10000, which corresponds to a bulk flow rate of $3.12\times10^{-4}\ kg/s$.

4. Numerical model

Since turbulent eddies are three-dimensional and unsteady, Large Eddy Simulations of turbulent flows should be carried out as 3D unsteady simulations. However, homogeneous and isotropic turbulence makes the quasi-3D LES capable of providing valuable information on the physics of turbulence [33]. On the other hand, although all turbulent flows include 3D instabilities under normal circumstances, some flow geometries with certain body forces can provide natural situations in which a flow may attain a quasi-3D configuration [34]. It has been shown that while quasi-3D LES of turbulent flows does not match to the real physics of turbulent eddies, it can provide wealthy qualitative and even quantitative information on the actual 3D phenomena [35, 36].

In the present case study, the flame can be assumed almost symmetry with respect to the axis. Therefore, a quasi-3D axisymmetric domain as shown in Fig. 2 is constructed. The computational domain is discretized with 491×1291 cells in radial and axial directions, respectively, constructing structured quadrilateral cells with 0.1 to 0.3 mm length in both directions. Setting up time-step size equal to 1×10^{-5} seconds and calculating the characteristic velocity scale based on the turbulent velocity fluctuations ($u' = (2k/3)^{0.5}$) the CFL number ($= u'\Delta t/\Delta x$) obtained between 0.4 to 1.3 through the computational domain. Normally, the time-step size in LES is selected somehow to provide CFL number around 1 so that all turbulent fluctuations down to the grid-scale eddies are resolved properly [37]. Like the grid independency task in RANS approach, proper choice of filter width across the computational domain is a crucial aspect of LES modeling and has a great impact on the accuracy of predictions. Based on principle of kinetic energy resolution, Celik et al. [38] proposed a quality index using the eddy viscosity ratio:

$$LES\_QI = \frac{1}{1+0.05\left(\mu_{eff}/\mu\right)^{0.53}} \quad (10)$$

where, $\mu_{eff} = \mu + \mu_t$ is the effective viscosity and μ is the laminar viscosity. According to Celik *et al.* [38], the LES quality index should be above 0.8 for quality of LES mesh. The quality index in the mesh grid constructed in this study shows almost uniform distribution between 0.91 to 0.95 throughout the computational domain. Typical value of 0.7 is considered for turbulent Prandtl and Schmidt numbers.

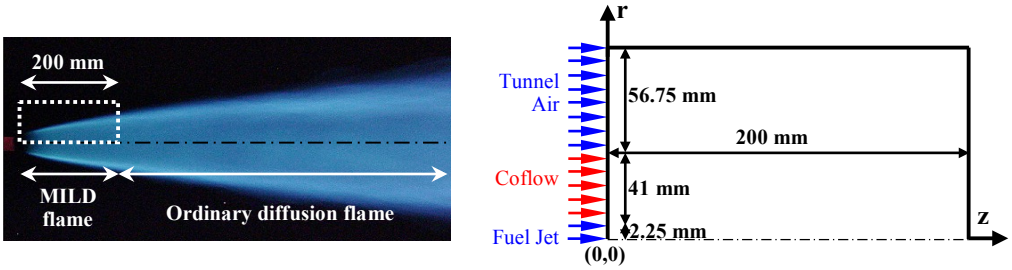

Fig. 2. Structure of the HM3 flame and the quasi-3D axisymmetric computational domain

Computations are conducted on a cluster of 24 cores (2×Intel Xeon 5645, 2.6 GHz, 24 GB RAM) within approximately three months comprising the solution of 12 equations (continuity, velocity components, energy, turbulent dissipation rate, radiation and six species concentration equations) on more than 633k computational nodes for 0.2 seconds of flow time with 20 internal iterations in each time step. Fuel oxidation was modeled using a reduced three-step chemical mechanism which has been previously verified for modeling of turbulent diffusion flames [39]:

$$\begin{aligned} CH_4 + 3/2\,O_2 &\rightarrow CO + 2H_2O & -r_{CH_4} &= 5.012\times10^{11} exp(-2.0\times10^8/RT)[CH_4]^{0.7}[O_2]^{0.8} \\ CO + 1/2\,O_2 &\rightarrow CO_2 & -r_{CO} &= 2.239\times10^{12} exp(-1.7\times10^8/RT)[CO][O_2]^{0.25} \\ H_2 + 1/2\,O_2 &\rightarrow H_2O & -r_{H_2} &= 9.870\times10^{8} exp(-3.1\times10^7/RT)[H_2][O_2] \end{aligned} \quad (11)$$

Turbulence-chemistry interaction was handled through the Finite Rate/Eddy Dissipation (FR/ED) model of Spalding [40]. It should be noted that combination of a global chemistry

scheme with FR/ED model is not the best approach for treating MILD combustion behaviors such as minor species prediction [10, 13] or extinction phenomenon [41]. In other words, application of detailed chemical mechanisms which involve several radical species with corresponding chain branching/propagation reactions has a substantial impact on prediction of pollutants emission or ignition delay but does not affect the mean temperature field or major species production. As the main goal of the present study is to determine the appropriate SGS model for treating temperature fluctuations in shear layers of JHC configurations, application of low-cost combustion models could reduce simulation time by several orders of magnitude.

LES results depend strongly on the appropriate choice of initial and boundary conditions. A preliminary RANS simulation was imposed on the high resolution grid, described above, and employed as an initial guess for further simulations. It has been observed that to avoid very long simulation time and finally numerical divergence, generating realistic instantaneous field is a mandatory stage before starting LES. The spectral synthesizer method was used to generate the instantaneous velocity from the mean values obtained using the steady-state RANS results. This method is based on the Random Flow Generation (RFG) technique proposed by Smirnov *et al.* [42] which applies Fourier transformation on the continuous flow-field to generate superposition of 100 harmonic functions. To account for consistency, the same method of spectral synthesizer which was used to generate initial random flow field was employed to impose transient inflow boundary conditions for all three inlet streams. It is worth noting that, applying different methods for initial flow field and inflow boundary conditions may result in numerical instabilities and finally divergence of computations. Finally, it should be noted that the transient initial and boundary conditions require realistic inlet conditions such as mean velocity field together with the turbulent production/dissipation rate of kinetic energy which can be obtained from a

preliminary converged RANS simulation. Unrealistic or flat turbulent profiles will generate unrealistic turbulent eddies at the inlets and throughout the flow field [43].

5. Results and discussion

In this section, results of LES calculations on the assessment of the four SGS models, described in previous sections are presented. Statistical data are collected at t = 0.124 s which corresponds to about 36 and 2 flow-through times for fuel-jet and coflow streams, respectively. In large eddy simulation of JHC flames coupled with global chemical mechanisms, reasonable prediction of mean species and temperature fields are the backbone for subsequent interpretation of fluctuating fields. Therefore, in section 5.1 a conceptual method is provided to assess SGS models based on detailed review of characteristics related to the mean values of major combustion products. Quantitative comparison for mean and fluctuating (*rms*) radial temperature profiles are then provided in section 5.2. The structure of mean, fluctuating and instantaneous temperature fields are also investigated qualitatively in the last section.

5.1. Conceptual analysis of the mean values of major products

Fig. 3 shows a typical profile for mean values of major products vs. mixture fraction appearing in JHC flames. According to Fig. 3, conceptual analysis of *x-y* plots for major combustion products vs. mixture fraction may result in five characteristics as follows:

1. *magnitude of peak value* which defines flame intensity;
2. *position of peak value* which corresponds to flame width;
3. *slope of rich-side* which is a measure of rich-side flame thickness;
4. *slope of lean-side* which represents penetration rate of laminar hot and diluted coflow into turbulent jet via large eddies developed in the mixing shear layer;

5. *intercept of major species mass fraction* which reveals no combustion occurrence using deficient oxygen in diluted coflow leading to stabilize a strong lifted tight jet flame instead of a wide MILD flame.

Based on the conceptual analysis of major products vs. mixture fraction described above and depicted in Fig. 3, the features of four static and dynamic SGS models will be evaluated using experimental observations reported for the HM3 flame.

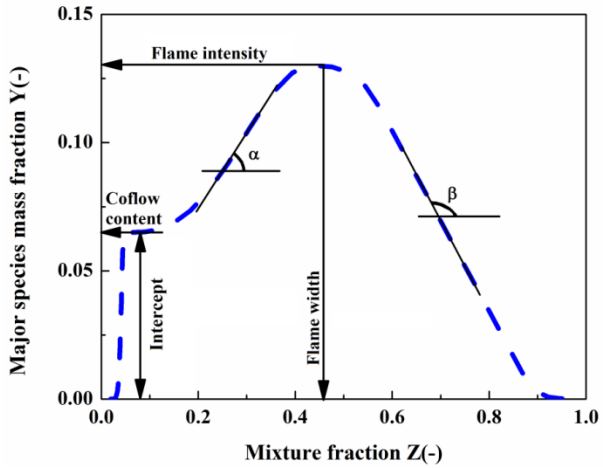

Fig. 3. Schematic distribution of major combustion products in the mixture fraction field

5.1.1. Magnitude of peak value

Distributions of experimental and numerical CO_2 and H_2O contents at three axial locations in the HM3 flame are illustrated in Fig. 4. Using the systematic conceptual analysis described above it can be inferred that flame intensity is partly under predicted due to the average over prediction of CO_2 and H_2O peaks obtained with both constants of the Smagorinsky model. In other words, higher amounts of major products predicted from a constant amount of fuel acts like a heat sink (to warm up more combustion products) and results in lower flame temperature. The dynamic Smagorinsky model well predicts peak value of CO_2 while notably underpredicts maximum values of H_2O. The dynamic kinetic energy model, however, resulted in reasonable peak values of CO_2 and H_2O combustion products.

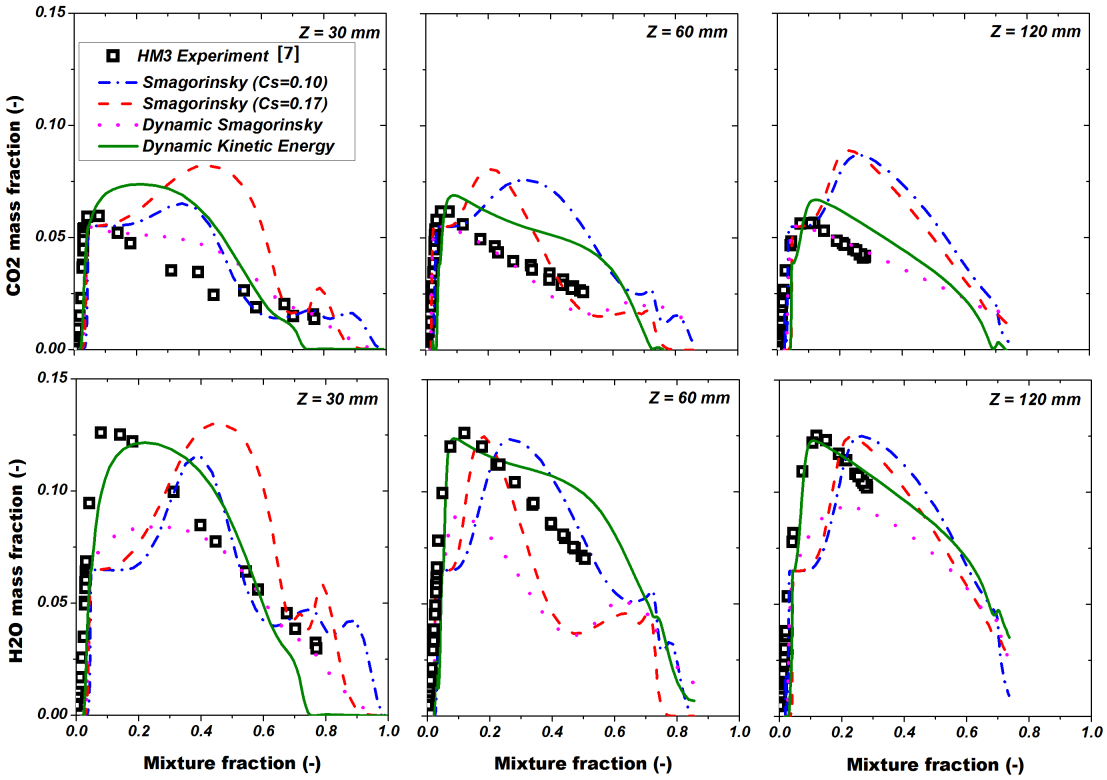

Fig. 4. Comparison of SGS models in prediction of major combustion products in the mixture fraction space

5.1.2. Position of peak value

According to schematic representation in Fig. 3, small values of mixture fraction related to the peak position of major products deal with volumetric torch-like flames, while larger values of mixture fraction represent tight jet-like flames. Inspection of Fig. 4 reveals that the Smagorinsky model with both static constants ($C_s = 0.10\ and\ 0.17$) resulted in tight jet-like flames while both dynamic SGS models show a wider flame which is in a good physical agreement with the volumetric HM3 flame experiment.

5.1.3. Slope of rich-side

According to Fig. 3 steep slope of rich-side describes a thin flame while a slight or gentle slope represents development of a thick flame. Fig. 4 shows that the flame thickness predicted by

the static Smagorinsky models is thinner than the experimental observations at all axial locations. However, the dynamic SGS models predicted more similar changes in CO_2 and H_2O production in the rich-side mixture fraction field.

5.1.4. Slope of lean-side

As mentioned before, profiles of CO_2 and H_2O mass fractions on the rich-side of JHC flames represent the amount of combustion products while their variation rates on the lean-side reveal dilution level of the hot coflow. According to Fig. 3 steep slope of lean-side represents thin mixing shear layer between the coflow and flame front. However, a gentle slope of the lean-side represents development of a wide mixing shear layer due to well penetration of laminar hot and diluted coflow into turbulent jet via large scale structures. Fig. 4 illustrates that only the dynamic models are able to capture a physical behavior of the lean-side which comes from dynamic assignment of model constants in the overlap between turbulent jet and laminar coflow. A closer look at the range of model constant assigned by the dynamic SGS models is illustrated in Fig. 5. It can be seen that the dynamic Smagorinsky model provided a sparse distribution of model constant in the range of 0 to 0.053. The DKE model, however, predicted a wide range of model constant from 0 to 0.230 around the mixing and thermal shear layers. This arises from the "non-local equilibrium" characteristic of the DKE model which enables it to assign a wide range of model constant for laminar and turbulent regions interconnecting around the mixing shear layer between laminar coflow and turbulent jet flame.

5.1.5. Intercept of major species mass fraction

The intercept of major products varying from coflow contents to higher values in the lean-side reveals that the SGS model is unable to predict a well-developed thick flame. In other words, moving from the tunnel-air flow towards the fuel jet at a constant axial location, the

mixture fraction varies from zero to one. Along this line, according to Fig. 4, the CO_2 and H_2O contents are zero in the tunnel-air flow ($z = 0$) and passing from coflow contents reach to the flame generated contents (z corresponding to Y_{max}). A closer look at the Fig. 4 two typical variations of the major products may be obtained by different SGS models. First behavior is uniform ascending contents of CO_2 and H_2O in the coflow region (Fig. 6a) predicted by dynamic SGS models which represents a well-developed thick flame. Second behavior is sudden change of CO_2 and H_2O mass fractions from the coflow contents to higher values (Fig. 6b) which represents a thin flame constricted around the center line. Fig. 4 illustrates that a tightened thin flame is systematically predicted by the static Smagorinsky model at all axial locations. However, the dynamic SGS models are able to predict a uniform ascending manner (like the experimental observations) from coflow contents to higher values of flame zone stabilized in a wider radius. A possible explanation for this phenomenon might be found in reasonable prediction of oxygen entrainment from deficient laminar coflow into the turbulent jet flame around the mixing shear layer via non-equilibrium assumption of dynamic SGS models.

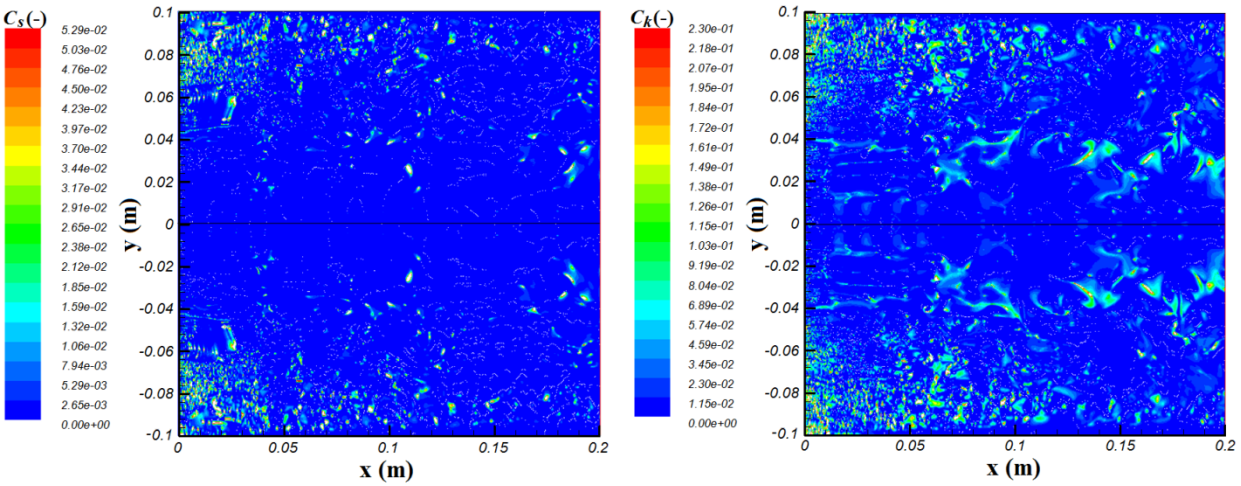

Fig. 5. Sub-grid eddy viscosity coefficient assigned by the (left) dynamic Smagorinsky and (right) dynamic kinetic energy models

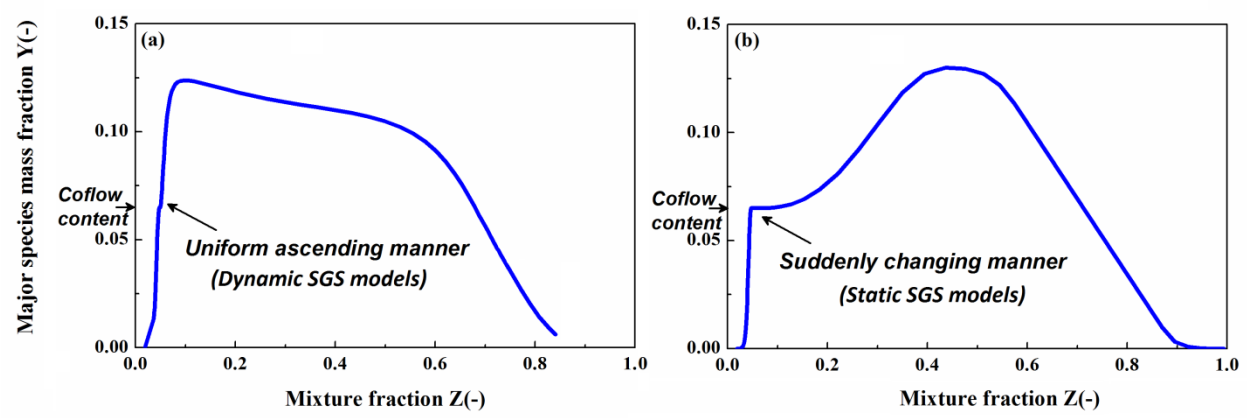

Fig. 6. Typical mass fraction of major species along the lean-side of the coflow region predicted by static and dynamic SGS models

5.2. Effect of SGS models on statistical temperature field

Profiles of mean temperature vs. mixture fraction predicted by different SGS models at three axial locations are illustrated in Fig. 7. For the mean temperature field the Smagorinsky model shows almost the same attitude with both constants; *e.g.* the peak temperature is under predicted by about 350 K. The dynamic Smagorinsky model also shows about 400 K under prediction of mean peak temperature. Inspection of the sub-grid dynamic Smagorinsky constant revealed that C_s was predicted up to 0.053 around the reaction zone which may be too low. According to Fig. 7 the dynamic kinetic energy (DKE) model provided best results for the mean value of peak temperature at all locations. The reason may be attributed to the local non-equilibrium assumption between the transferred energy through the grid-filter scales and its dissipation at small sub-grid scales. The other reason may come from assigning proper sub-grid dynamic viscosity constant C_k up to 0.23 in reaction zone region as illustrated in Fig. 5.

As can be seen in Fig. 7, the DKE model, like the static and dynamic Smagorinsky models, tends to produce faster reaction zone near the center, leading to small shift of peak temperature

towards the fuel lean-side. The sub-grid turbulent viscosity predicted by dynamic SGS models is about two orders of magnitude smaller than that predicted by static SGS models. Panjwani *et al.* [44] obtained similar results when comparing dynamic and static Smagorinsky models on the LES of Sandia Flame D. They claimed that this issue resulted to accelerated peak temperature predicted by dynamic Smagorinsky model. As a matter of fact, we cannot corroborate this statement, since both static and dynamic SGS models, studied here, have predicted almost similar position of the reaction zone in JHC configuration (see Fig. 7).

It should be noted that the discrepancies obtained in all SGS models at the fuel rich-side of the mixture fraction space are due to poor mixing predicted in the mixing shear layer which may be partly attributed to the axisymmetric boundary condition imposed on the center line. This can lead to disturbing computation of asymmetric turbulent structures around the center line region [36]. Therefore, improvement of these results is possible with full 3D LES computations considering a more realistic asymmetric turbulent flow around the center line region. Similar conclusion may be drawn for deviation of mean values of major products in the rich-side depicted in Fig. 4.

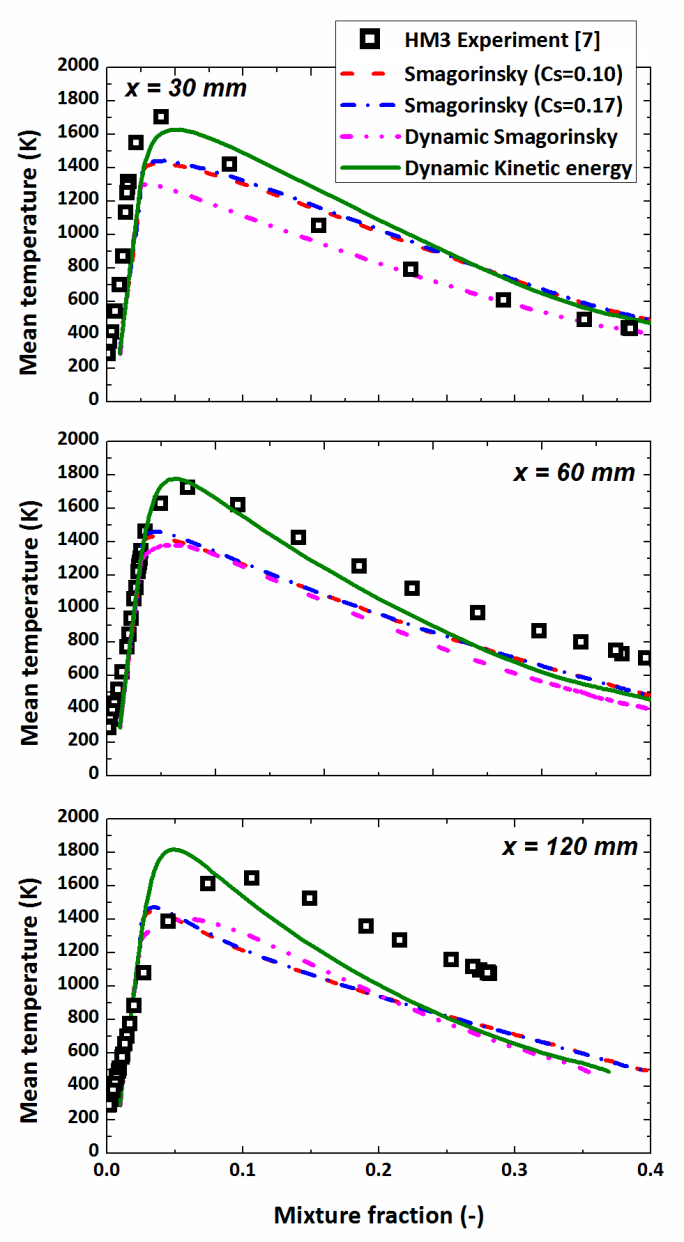

Fig. 7. Comparison of different SGS models on prediction of mean temperatures vs. mixture fraction at various axial locations

In accordance with the mean temperature field, the DKE model provided better accuracy for prediction of the temperature fluctuations in shear layers as shown in Fig. 8. Although, the long simulation time to get statistically stationary results is hampered by the un-affordable computational cost, results of temperature fluctuations in shear layers obtained with the DKE

model are satisfactory. Hence, it can be concluded that the prediction of the dynamic SGS models is, noticeably, better than that of the static SGS models.

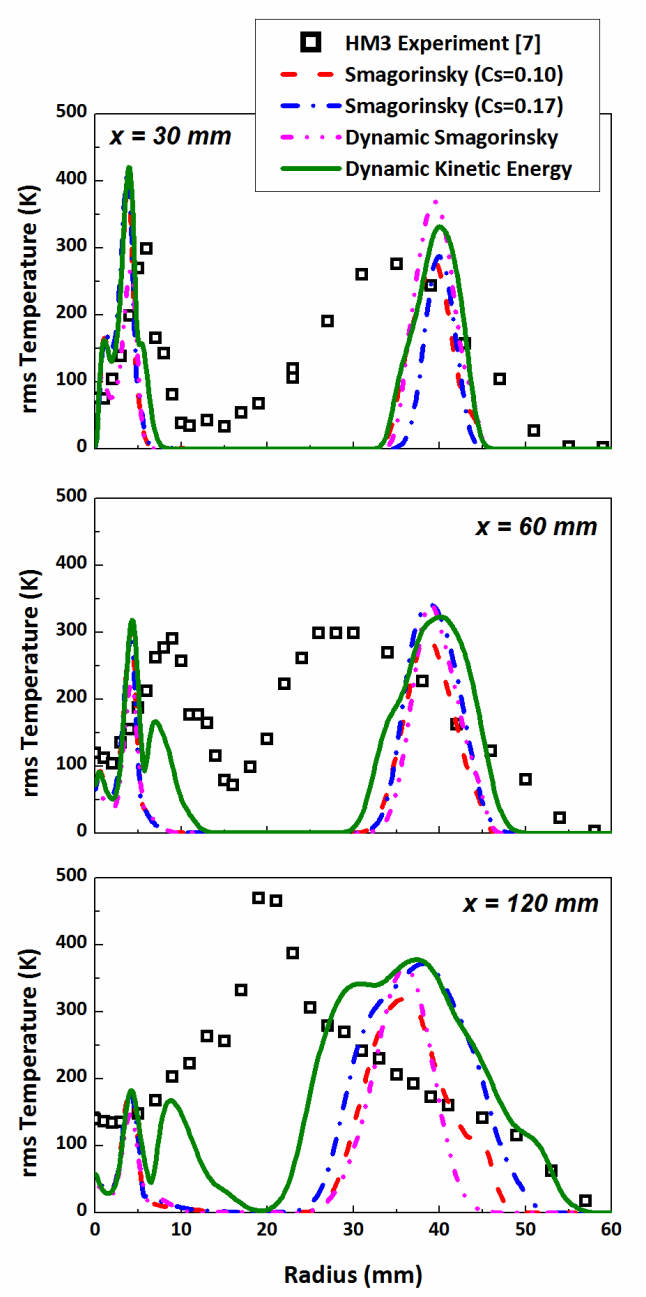

Fig. 8. Comparison of different SGS models on predicting radial profiles of temperature fluctuations at various axial locations

A comparison of predicted temperature fluctuations in shear layers with those of reported in recent numerical studies on the HM3 flame is presented in Fig. 9. As can be seen, the magnitude of the first peak corresponding to the mixing shear layer is partly over-estimated compared with the two previous studies.

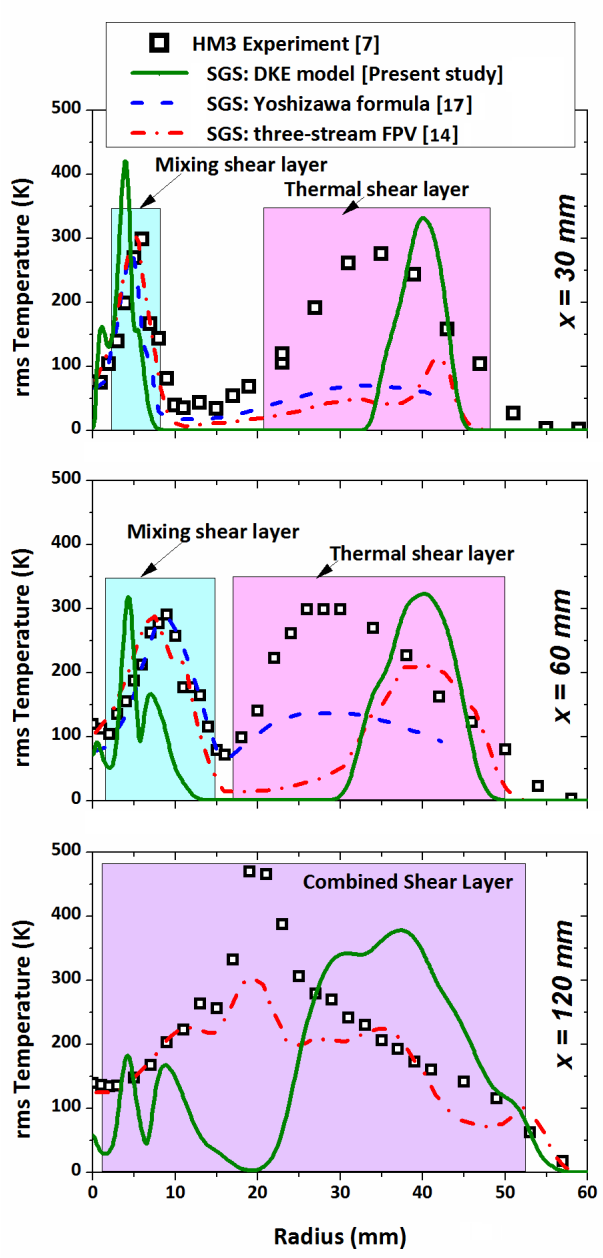

Fig. 9. Comparison of predicted temperature fluctuations in shear layers with previous LES studies

The axisymmetric boundary condition imposed on the center line of the present study might be responsible for partial over-prediction of temperature fluctuations in the mixing shear layer. In the thermal shear layer, it can be seen that the second peak is under-estimated by about 200 K in previous works [19, 22]. Unlike the previous studies, the magnitude of the second peak at $z = 30$ and 60 mm, is properly captured by the DKE SGS model. Predicted peak value of the combined shear layer at downstream ($z = 120\,mm$) is also slightly improved rather than the numerical results of previous studies. The peak positions are slightly over-estimated especially at upstream, as observed in similar studies [19] which the reason is not clear yet. It should be noted that improved results of temperature fluctuations in the present study have been obtained using the simple FR/ED combustion model coupled with a global three-step chemical mechanism. These findings highlight the importance of applying dynamic SGS models for JHC flames and anticipate that much improved results could be pursued if the DKE SGS model is employed with more accurate combustion and chemistry models.

5.3. Structure of temperature field

Qualitative comparisons of instantaneous and fluctuating temperature fields obtained at t = 0.124 s using static and dynamic SGS models are presented in Figs. 10 and 11. Results of static Smagorinsky model, presented in Fig. 10, reveal no significant differences in the temperature fields with constant coefficients of 0.10 and 0.17. In particular, the maximum values of intantaneous and *rms* temperatures are almost the same. More importantly, the width and magnitude of temperature fluctuations in mixing and thermal shear layers are almost similar. This indicates that changing Smagorinsky constant from a conservative value ($C_s = 0.10$) to higher values ($C_s = 0.17$), which is normally suggested for homogeneous isotropic turbulence [29], has not a great influence on resolving shear layers structure. In other words, application of

static SGS models which assign a single constant eddy viscosity coefficient throughout the laminar, transient and turbulent regions of JHC structures is not suitable.

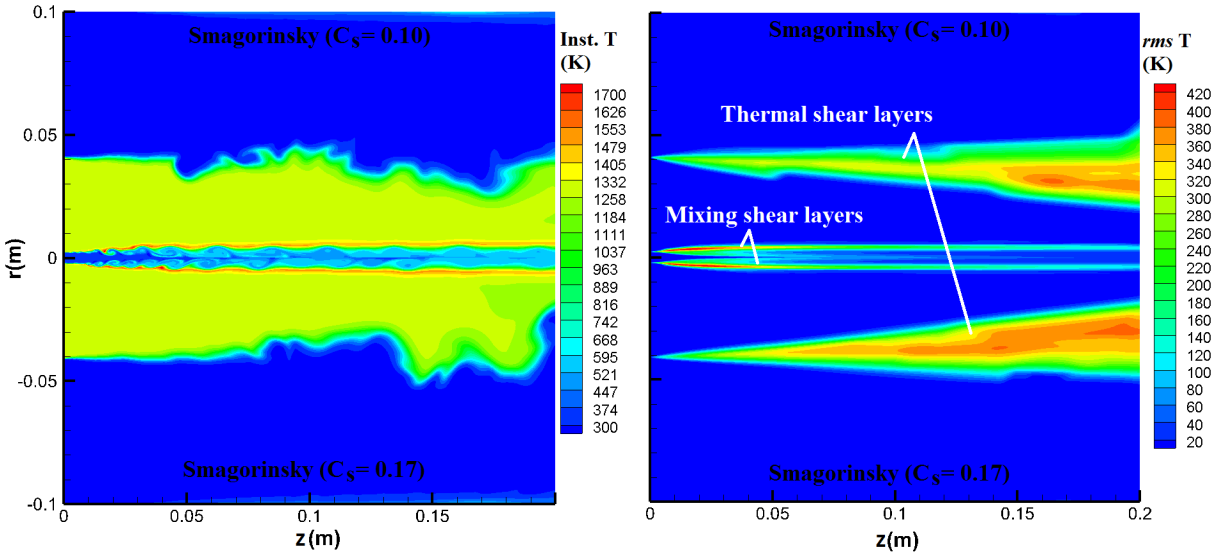

Fig. 10. Instantaneous and Fluctuating temperature fields predicted by the Smagorinsky SGS model

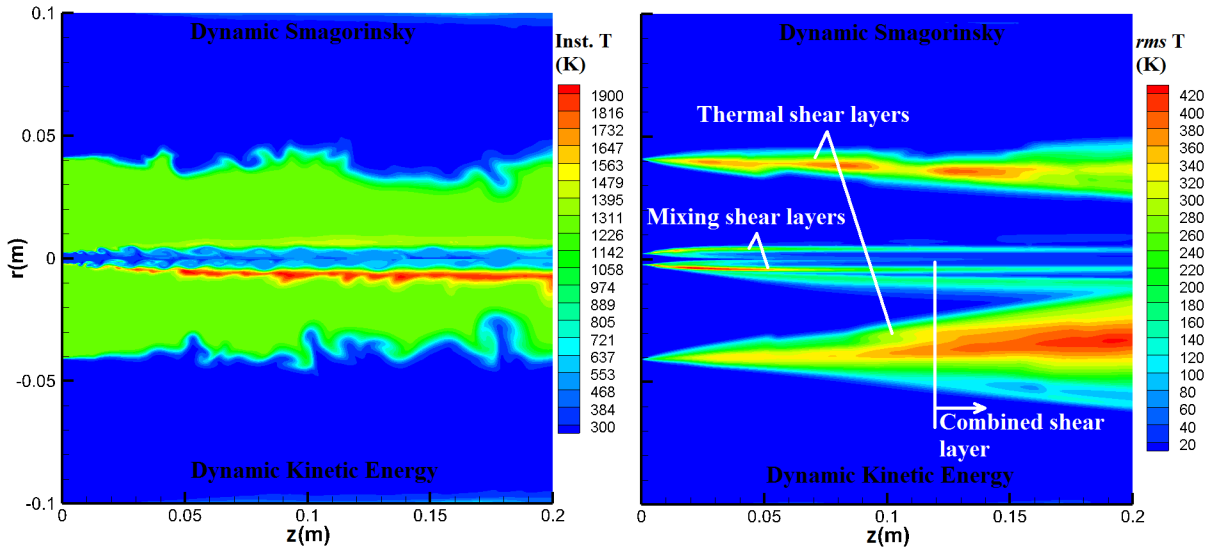

Fig. 11. Instantaneous and fluctuating temperature fields predicted by the DS and DKE SGS models

According to Fig. 11, the dynamic Smagorinsky (DS) model shows a large under-estimation of the peak temperature, while the dynamic kinetic energy (DKE) model provides reasonable predictions in both instantaneous and mean temperature fields. It can be seen that both simulations confirm the experimental observation of temperature fluctuations in the mixing and thermal shear layers. However, both mixing and thermal shear layers have predicted clearly wider in the DKE model demonstrating well development of mixing between fuel jet and coflow as well as between coflow and tunnel air flows toward downstream. The DKE sub-grid scale model which solves a transport equation for turbulent kinetic energy can consider the history and non-local effects in laminar coflow and tunnel air streams as well as in turbulent fuel-jet. Therefore, turbulent kinetic energy produced by large scale structures in the turbulent fuel-jet can transport through the transient mixing and thermal shear layers and dissipate physically elsewhere. In addition, dynamic assignment of eddy viscosity coefficient in the DKE model can provide physical values through the interconnected laminar and turbulent regions. These superiorities show that the DKE model is able to physically capture development of mixing and thermal shear layers. Comparing shear layers in Figs. 10 and 11 elucidates that only the DKE model can successfully predict interconnection between mixing and thermal shear layers via development of the combined shear layer at downstream. This shows that the dynamic kinetic energy model with its non-equilibrium turbulence assumption is the best fitted SGS model for the JHC flames as it can provide improved accuracy on developing mixing and thermal shear layers over the other sub-grid scale models.

Conclusions

Large Eddy Simulation (LES) of a hydrogen/methane JHC flame is conducted by using static and dynamic sub-grid scale (SGS) models, in order to investigate their predictive

performance on the resolution of complex flame structure. A conceptual analysis of the mean values of major combustion products has been performed to investigate JHC flame characteristics with various SGS models. It is shown that the mean values of major products obtained from a simplified combustion model coupled with a global chemistry can provide significant information on the volume and intensity of JHC flames. Quantitative and qualitative comparison with experimental data on the mean and fluctuating temperature clearly demonstrated that dynamic SGS models can successfully capture physics of shear layers in JHC flame. In particular, temperature fluctuations between shear layers are well predicted by the dynamic kinetic energy model. The quasi-3D LES conducted in this study, while does not match to the real physics of turbulent JHC flames, can provide wealthy qualitative and even quantitative information on mixing and temperature fluctuations in shear layers. Present results are valuable for further full 3D-LES with detailed chemistry to explore the influence of scalar fluctuations on the complex features of JHC flames such as local extinction and pollutant emissions.

Acknowledgments

Present research was financially supported by the Research Center of the Shahid Beheshti University (SBU). We are thankful to the SBU cluster "SARMAD" officials which provided access to a high performance computing system.

References

[1] A. Cavaliere, and de M. Joannon, Mild combustion, Prog. Energy Combust. Sci. 30 (2004) 329–366.

[2] R.S. Rogallo, and P. Moin, Numerical simulation of turbulent flows, Ann. Review Fluid Mech 16 (1984) 99–137.

[3] P.E. DesJardin, and S.H. Frankel, Large Eddy Simulation of a Non-premixed Reacting Jet: Application and Assessment of Subgrid-Scale Combustion Models, Phys. Fluids 10 (1998) 2298–2314.

[4] J.A. Wünning, and J.G. Wünning, Flameless oxidation to reduce thermal NO formation, Prog. Energy Combust. Sci. 23 (1997) 81–94.

[5] H. Tsuji, A.K. Gupta, T. Hasegawa, M. Katsuki, K. Kishimoto, and M. Morita, High temperature air combustion: from energy conservation to pollution reduction. CRC Press, 2003.

[6] M. Flamme, New combustion systems for gas turbines (NGT), Appl. Therm. Eng. 24 (2004) 1551–1559.

[7] B.B. Dally, A.N. Karpetis, and R.S. Barlow, Structure of turbulent nonpremixed jet flames in a diluted hot coflow, Proc. Combust. Inst. 29 (2002) 1147–1154.

[8] A. Rebola, M. Costa, P. J. Coelho, Experimental evaluation of the performance of a flameless combustor, Appl. Therm. Eng. 50 (2013) 805–815.

[9] S.R. Shabanian, P.R. Medwell, M. Rahimi, A. Frassoldati, A. Cuoci, Kinetic and fluid dynamic modeling of ethylene jet flames in diluted and heated oxidant stream combustion conditions, Appl. Therm. Eng. 52 (2013) 538–554.

[10] S.H. Kim, K.Y. Huh, and B.B. Dally, Conditional moment closure modeling of turbulent nonpremixed combustion in diluted hot coflow, Proc. Combust. Inst. 30 (2005) 751–757.

[11] F.C. Christo, and B.B. Dally, Modeling turbulent reacting jets issuing into a hot and diluted coflow, Combust. Flame 142 (2005) 117–129.

[12] J. Aminian, C. Galletti, S. Shahhosseini, and L. Tognotti, Key modeling issues in prediction of minor species in diluted-preheated combustion conditions, Appl. Therm. Eng. 31 (2011) 3287–3300.

[13] J. Aminian, C. Galletti, S. Shahhosseini, and L. Tognotti, Numerical investigation of a MILD combustion burner: Analysis of mixing field, chemical kinetics and turbulence-chemistry interaction, Flow, Turbulence Combust. 88 (2012) 597–623.

[14] M. Ihme, and Y.C. See, LES flamelet modeling of a three-stream MILD combustor: Analysis of flame sensitivity to scalar inflow conditions, Proc. Combust. Inst. 33 (2011) 1309–1317.

[15] M. Klein, A. Sadiki, and J. Janicka, A digital filter based generation of inflow data for spatially developing direct numerical or large eddy simulations, J. Computational Physics 186 (2003) 652–665.

[16] M. Ihme, J. Zhang, G. He, and B.B. Dally, Large-eddy simulation of a jet-in-hot coflow burner operating in the oxygen-diluted combustion regime, Flow Turbul. Combust. 89 (2012) 449–464.

[17] Y. Afarin, and S. Tabejamaat, Effect of hydrogen on H2/CH4 flame structure of MILD combustion using the LES method, Int. J. Hydrogen Energy 38 (2013) 3447–3458.

[18] H. Zhang, Z. Yu, T. Ye, M. Zhao, M. Cheng, Large eddy simulation of turbulent lifted flame in a hot vitiated coflow using tabulated detailed chemistry, Appl. Therm. Eng. 128 (2018) 1660–1672.

[19] Abtahizadeh E., de Goey P., van Oijen J. 2017, LES of Delft Jet-in-Hot Coflow burner to investigate the effect of preferential diffusion on autoignition of CH4=H2 flames, Fuel 191 (2017) 36–45.

[20] L.Y. Hu, L.X. Zhou, and Y.H. Luo, Large-Eddy Simulation of the Sydney Swirling Non Premixed Flame and Validation of Several Subgrid-Scale Models, Numer. Heat Tr. B-Fund. 53 (2008) 39–58.

[21] J. Smagorinsky, General circulation experiments with the primitive equations. I. The Basic Experiment, Monthly Weather Review 91 (1963) 99–164.

[22] O.J. McMillan, and J.H. Ferziger, Direct testing of sub-grid-scale models, AIAA J. 17 (1979) 1340–1346.

[23] D.K. Lilly, The representation of small-scale turbulence in numerical simulation experiments, In H. H. Goldstine (Ed.), Proc. IBM Scientific Computing Symp. on Environmental Sciences (1967) 195–210.

[24] U. Schumann, Direct and large eddy simulation of turbulence – summary of the state of the art, Lecture Series Introduction to the Modeling of Turbulence, Von Karman Institute, Brussels, 1991.

[25] J.W. Deardorff, On the magnitude of the sub-grid scale eddy viscosity coefficient, J. Computational Physics 7 (1971) 120–133.

[26] U. Piomelli, P. Moin, and J.H. Ferziger, Model consistency in the large eddy simulation of turbulent channel flows, Physics of Fluids 31 (1988) 1884–1891.

[27] P. Moin, and J. Kim, Numerical investigation of turbulent channel flow, J. Fluid Mechanics 118 (1982) 341–377.

[28] M. Germano, U. Piomelli, P. Moin, and W.H. Cabot, A dynamic sub-grid scale eddy viscosity model, Physics Fluids 3 (1991) 1760–1765.

[29] B. Vreman, B. Geurts, and H. Kuerten, Large eddy simulation of the turbulent mixing layer, J. Fluid Mechanics 339 (1997) 357–390.

[30] D.K. Lilly, A proposed modification of the Germano sub-grid-scale closure model, Physics of Fluids 4 (1992) 633–635.

[31] W.W. Kim, and S. Menon, Application of the localized dynamic sub-grid-scale model to turbulent wall-bounded flows, Technical Report AIAA-97-0210, 35th Aerospace Sciences Meeting, Reno, NV, 1997.

[32] S. Kim, Large eddy simulation using an unstructured mesh based finite-volume solver, 34th AIAA Fluid Dynamics Conference and Exhibit, Portland, Oregon, 2004.

[33] S. James, and F.A. Jaberi, Large Scale Simulations of Two-Dimensional Non-Premixed Methane Jet Flames, Combust. Flame 123 (2000) 465–487.

[34] S. Sukoriansky, A. Chekhlov, S.A. Orszag, B. Galperin, and I. Staroselsky, Large eddy simulation of two-dimensional isotropic turbulence, J. Scientific Computing 11 (1996) 13–45.

[35] C. Lian, C.L. Merkle, and G. Xia, Flow field initialization and approach to stationary conditions in unsteady combustion simulations, Computers Fluids 39 (2010) 310–323.

[36] J. Schlüter, Influence of axisymmetric assumptions on Large Eddy Simulations of a confined jet and a swirl flow, Int. J. Computational Fluid Dynamics 18 (2004) 235–245.

[37] A. Sadiki, B. Maltsev, F. Wegner, A. Flemming, and J. Janicka, Unsteady methods (URANS and LES) for simulation of combustion systems, Int. J. Thermal Sciences 45 (2006) 760–773.

[38] I. Celik, Z. Cehreli, and I. Yavuz, Index of resolution quality for large eddy simulation, J. Fluids Eng. 127 (2005) 949–958.

[39] J. P. Kim, U. Schnell, G. Scheffknecht, Comparison of different global reaction mechanisms for MILD combustion of natural gas, Combust. Sci. and Tech. 180 (2008) 565–592.

[40] D.B. Spalding, Mixing and chemical reaction in steady confined turbulent flames, Proc. Combust. Inst. 13 (1971) 649–672.

[41] J. Aminian, C. Galletti, and L. Tognotti, Extended EDC local extinction model accounting finite-rate chemistry for MILD combustion, Fuel 165 (2016) 123–133.

[42] R. Smirnov, S. Shi, and I. Celik, Random flow generation technique for Large Eddy Simulations and particle-dynamics modeling, J. Fluids Eng. 123 (2001) 359–371.

[43] Inlet boundary conditions for the LES model, ANSYS Fluent 12.0 help document.

[44] B. Panjwani, I.S. Ertesvg, K.E. Rian, and A. Gruber, Sub-grid combustion modeling for large eddy simulation (LES) of turbulent combustion using eddy dissipation concept. in: 5th European Conference on Computational Fluid Dynamics, ECCOMAS CFD 2010, Lisbon, Portugal, 2010.